# Reconstruction of Holocene monsoon history from the Pearl River Estuary, southern China, using diatoms and carbon isotope ratios

Y. Zong,[1*] J.M. Lloyd,[1] M.J. Leng,[2] W.W.-S. Yim[3] and G. Huang[3]

*([1]Department of Geography, University of Durham, South Road, Durham DH1 3LE, UK; [2]NERC Isotope Geosciences Laboratory, British Geological Survey, Nottingham NG12 5GG, UK and School of Geography, University of Nottingham, Nottingham NG7 2RD, UK; [3]Department of Earth Sciences, The University of Hong Kong, Hong Kong, SAR, China)*

Received 10 January 2005; revised manuscript accepted 25 August 2005

A HOLOCENE RESEARCH PAPER

**Abstract:** This study employs a multiproxy approach in the reconstruction of Holocene monsoon history from sedimentary sequences obtained from the Pearl River Estuary, southern China. A set of modern surface sediment samples were collected within and outside the estuary, and a sediment core was obtained from the mouth of the estuary. A range of modern environmental variables were recorded including water salinity (summer, winter and annual average) and water depth. The diatom results show a good relationship with water salinity, with marine diatoms dominating the more distal samples from outside the main estuary and freshwater diatoms dominating the proximal samples influenced by higher freshwater flux. This pattern is matched by the bulk organic carbon isotopes. The isotope values vary between $-21.1\pm0.3$‰ for samples from the fully marine environment, between $-23.2\pm0.8$‰ and $-23.7\pm0.8$‰ for samples from the mid to outer estuary brackish water environment and less than $-24.7\pm1.3$‰ for samples from the inner estuary close to the freshwater sources. Similarly, the C/N ratios vary from below $7\pm0.6$ in the marine end-members to over $14.8\pm3.0$ in the freshwater end-members. Both the diatom and carbon data from the sediment core reveal a significant increase in freshwater flux from 8500 cal. yr BP resulting from the enhanced summer monsoon regime in early Holocene. The strength of freshwater flux reached its highest between 7500 and 6000 cal. yr BP. In the last 6000 years, freshwater flux decreased towards present, reflecting a gradual weakening of the summer monsoon.

**Key words:** East Asian monsoon, freshwater flux, diatoms, carbon isotopes, modern environment, Holocene, Pearl River Estuary, southern China.

## Introduction

The East Asian Monsoon (EAM) system is an important component of the global climate system. Regionally, it is one of the key factors controlling environmental conditions and supports a highly productive ecosystem. It is also socio-economically important in the densely populated East Asia region where flood and drought hazards are common. Globally, previous studies have identified teleconnections between the EAM and phenomena in other regions such as the North Atlantic Oscillation (NAO), El Niño–Southern Oscillation (ENSO) and even the North Atlantic thermohaline circulation (THC) (eg, Shukla and Paolina, 1983; Yang, 1996; Overpeck *et al.*, 1996; Sirocko *et al.*, 1996). The EAM system forms a key part of the global atmospheric circulation. Thus an understanding of the past variability of the EAM is of great importance in understanding possible future changes.

The majority of studies of Holocene Asian monsoon variability are based on reconstructions derived from loess records (eg, An *et al.*, 1993), marine records (eg, Huang *et al.*, 1997; Wang *et al.*, 1999a,b; Sarkar *et al.*, 2000) and lake records (eg, Lister *et al.*, 1991; Lou and Chen, 1997; Chen

*Author for correspondence (e-mail: y.q.zong@durham.ac.uk)



10.1191/0959683606hl911rp

*et al.*, 1999). There are also a limited number of records from ice cores, stalagmites, tree rings and maar lakes (Thompson *et al.*, 1989, 2000; Burns *et al.*, 1998; Feng *et al.*, 1999; Denniston *et al.*, 2000; Chu *et al.*, 2002; Zhang *et al.*, 2004). The research presented here for the first time investigates the potential for estuarine records to be used to reconstruct the Holocene history of EAM variability. We test the hypothesis that palaeoenvironmental proxies from an estuarine environment can be closely related to fluctuations in freshwater discharge associated with monsoon variability. Long-term changes in monsoon strength result in fluctuations in the amount of precipitation and, hence, freshwater flux through major estuarine systems into the sea. We examine the range of carbon isotopes and C/N ratios from bulk organic matter, along with diatom flora from the contemporary estuarine environment to test the applicability of this methodology before applying it to a fossil sequence from the Pearl River Estuary.

The Pearl River Estuary was chosen for this investigation because of its latitude-orientated drainage basin which lies between 26°N and 22°N (Figure 1), a transitional region between tropic and temperate zones. The drainage basin is under the influence of humid summer monsoon from the south and dry winter monsoon from the north. Thus, the study area is highly sensitive to monsoon variability. Three main rivers (East River, North River and West River) drain into the drowned coastal basin and create two deltaic complexes that are separated by the estuary. The large hilly outcrops north of Macau and solid outcrops of Shenzhen and Hong Kong (Figure 2) have, to a certain extent, confined the development of the delta plains and the estuary, restricting its lateral movement. Therefore, sediment cores from the mouth of the estuary have the potential to provide reliable records of freshwater discharge from the drainage basin. Variations in the freshwater flux can then be related to the variability of the East Asian Monsoon.

## Methodological approach

This research aims to examine the potential of a multiproxy approach in the reconstruction of Holocene monsoon history from estuarine sediment sequences with an average sedimentation rate of 1.0 mm/yr at the mouth of the Pearl River Estuary at a resolution ranging from 20 to 50 years. Variations in monsoon intensity produce fluctuations in precipitation (An *et al.*, 1993) and freshwater flux through the Pearl River Estuary into the South China Sea. The key to this research thus lies in the link between freshwater flux and changing conditions preserved within the Pearl River Estuary. To establish the link between freshwater flux and environmental proxies, we investigate the modern environment within the estuary by examining a set of surface sediment samples from 40 locations covering the full range of environments from freshwater to fully marine conditions (Figure 2). These sediment samples provide environmental information averaged over several years (see next section). The spatial context of this contemporary data set allows us to investigate the changing proxy signature across the full salinity range from freshwater to fully marine water. Proximal sites with strong freshwater influence are used to represent conditions of intensified monsoon, whilst distal sites with weak freshwater influence are used to represent conditions of weakened monsoon. The modern relationship between our proxies, water salinity and freshwater influence can then be used to assess past changes in freshwater flux to the estuary based on a fossil sequence. This further analysis is based on the upper 10 m of a sediment core taken from the mouth of the Pearl River Estuary (Figure 2), in order to test the applicability of the methods in reconstruction of Holocene monsoon history.

Proxies employed in this study include carbon isotope and C/N ratios of bulk organic matter and diatom flora. The applicability of the diatom methodology relies on a direct link between the water salinity (influenced by changing freshwater flux) and flora. This is a well-established methodology. Diatom techniques have been used in many studies to reconstruct changes in water salinity and coastal evolution, often associated with sea-level changes (eg, Zong, 1992; Owen *et al.*, 1998; Fyfe *et al.*, 1999; Yim and Li, 2000). The applicability of carbon isotope and C/N ratios from bulk organic matter relies on our ability to identify the changing sources of organic material preserved in the estuarine sediments and to relate these to changes in freshwater flux to the Pearl River Estuary. The principal sources of organic material preserved in the estuarine environment are: terrestrial plant matter transported by the river flow to the estuary; freshwater algae transported to the estuary by the river flow; brackish water algal/aquatic plant material produced *in situ*; marine algal material produced *in situ* or carried in by marine water influx to the estuary (Figure 3). Changes in monsoon intensity will lead to significant

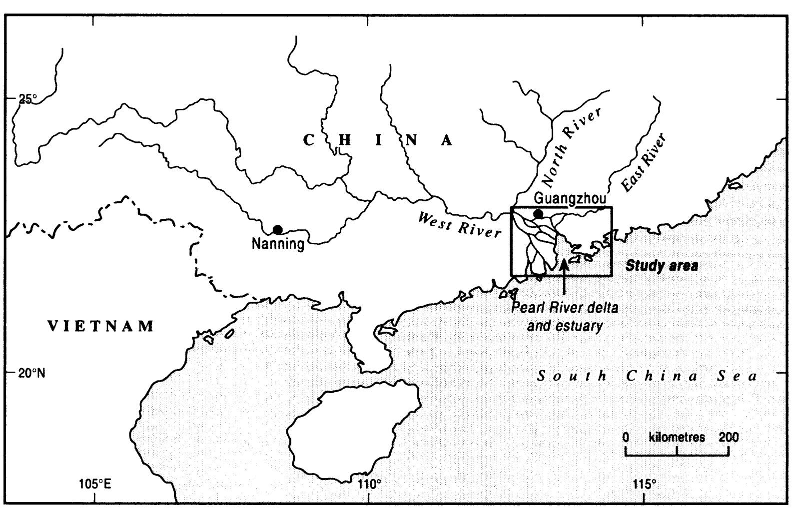


**Figure 1** Location of the Pearl River drainage basin, delta plain and estuary

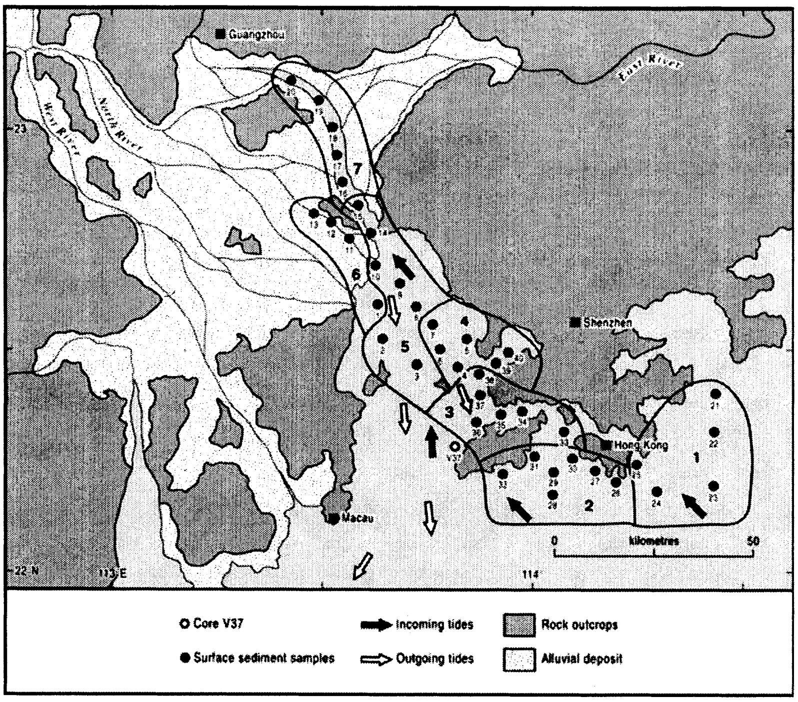


**Figure 2** The Pearl River delta plain and estuary, with locations of sampling points for present-day surface sediments and the sediment core. The sampling points are arranged into groups (1 to 7) based on the cluster analysis of diatom assemblages

changes in freshwater flux into the Pearl River Estuary and, associated with this, significant changes in the flux of organic material. For example, an increase in freshwater flux will result in an increase in terrestrial plant material and freshwater algae transported to and deposited in the estuary. Alternatively, a decrease in freshwater flux will reduce the quantity of freshwater algae and terrestrial plant material being transported to the estuary and also lead to an increase in water salinity enhancing the *in situ* productivity from brackish water algae.

The predominant source of the organic material can be estimated from the C/N ratios and $\delta^{13}C$ of organic material. This methodology has been applied widely to palaeoenvironmental reconstruction based on lake sediments (eg, Meyers and Ishiwatari, 1993; Meyers, 1994; Meyers and Teranes, 2001; Leng and Marshall, 2004; Lamb *et al.*, 2004). A number of studies have also used C/N ratios and $\delta^{13}C$ in estuarine and coastal environments as tracers of organic material (eg, Thornton and McManus, 1994; Middelburg and Nieuwenhuize, 1998; Müller and Mathesius, 1999) and to reconstruct palaeoenvironmental (salinity) change, (eg, Chmura and Aharon, 1995; Müller and Voss, 1999; Yamamuro, 2000;

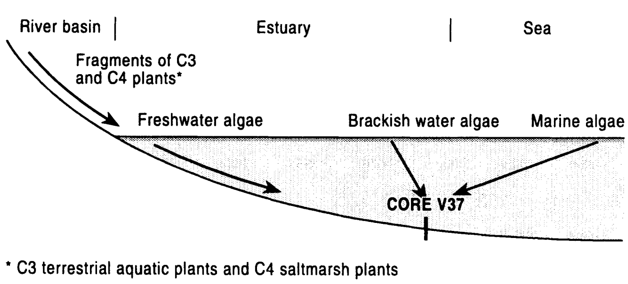


**Figure 3** Schematic diagram indicating possible sources of organic matter and their contributions to the sediment core

Müller, 2001; Bryne *et al.*, 2001; Westman and Hedenström, 2002; Mackie *et al.*, 2005; Wilson *et al.*, 2005).

The carbon isotopic composition of plants is variable and depends on the source of carbon assimilated. Terrestrial plants record $\delta^{13}C$ values ranging from $-13$ to $-30‰$, however C3 plants generally record values of $-23$ to $-30‰$, while C4 plants record values around $-13‰$ (Smith and Epstein 1971; Meyers, 1994). Most terrestrial plants have C/N ratios $>20$ (Meyers, 1994). Freshwater aquatic plants and plankton have $\delta^{13}C$ values ranging from $-25$ to $-30‰$, but are distinguishable from terrestrial plants by their low C/N ratios which are generally between 4 and 10 (Meyers, 1994). Marine plants have higher $\delta^{13}C$ values ranging from $-10$ to $-22‰$ (Boutton, 1991), although marine algae have $\delta^{13}C$ values ranging from $-20$ to $-25‰$ (Meyers, 1994). Marine bulk organic matter from surface sediments is usually dominated by algae, and in general has $\delta^{13}C$ values ranging from $-19$ to $-22‰$ (Fontugne and Jouanneau, 1987). C/N ratios from marine algae are generally $<10$ (Meyers, 1994). Organic carbon from estuarine environments, as described above, is produced by a mixture of allochthonous terrigenous and marine flux, and autochthonous estuarine matter. Suspended matter and sediments from estuaries in general have values between the end-member values from marine and freshwater environments. Thornton and McManus (1994) from the Tay Estuary record a shift in $\delta^{13}C$ ratios from between $-26$ and $-28‰$ in the upper estuary and freshwater locations, to $-23.2‰$ at the mouth of the estuary. Over this transect C/N ratios drop from between 10 and 20 in upstream sites to around 10 close to the estuary mouth. In a similar study of the Schelde Estuary, Middelburg and Nieuwenhuize (1998) identified a trend in $\delta^{13}C$ ratios from $-22$ to $-24‰$ at the estuary mouth to $-27‰$ 60 km upstream and a corresponding change in C/N ratio from 8 to 12 at the mouth to between 14 and 21 upstream.

## Material and methods

A grab sampler was used to obtain the top 10 cm of sediments from each site. Thus the samples potentially represent sediments deposited in the last 6–10 years according to the sedimentation rates of around an average 1.8 cm/yr on shoals within the estuary (Li *et al.*, 1991) and generally below 1.0 cm/yr from the area of Hong Kong (Owen, 2005). The sediment samples were stored in a sealed plastic container kept in a fridge. During sampling, water depth was measured (Table 1), and time recorded for back calculation against tidal cycles. The average tidal range for the area is between 1.30 m at the mouth and 1.90 m at the head of the estuary. Water salinity was recorded during sampling, and all measurements are comparable with the monthly data published by the Environmental Protection Department, HK SAR Government and by the Water Resource Committee for the Pearl River in Guangzhou (Table 1).

The sediment core was obtained through the Civil Engineering Department, HK SAR Government. Based on radiocarbon dating, the average sedimentation rate for the core is 1.47 mm/yr. Thus, each subsample, 1 cm thick, represents potentially a 7-yr mean record. The 6 cm sampling interval through the core will provide a data set with a 40-yr resolution. Sediment

**Table 1** Measurements for the 40 present-day surface sediment samples

| Sample number | Water depth (m) | TOC (%) | Water salinity (‰) | | Bulk organic $\delta^{13}C$ (‰) | C/N ratio | Diatom groups |
|---|---|---|---|---|---|---|---|
| | | | Summer | Winter | | | |
| PE17 | 2.1 | 8.7 | 1.6 | 8.6 | −26.6 | 20.1 | 7 |
| PE16 | 2.5 | 4.1 | 2.2 | 10.6 | −23.7 | 13.4 | |
| PE20 | 2.1 | 8.7 | 0.0 | 2.7 | −25.0 | 14.4 | |
| PE18 | 2.4 | 5.6 | 0.8 | 5.7 | −23.3 | 12.6 | |
| PE19 | 2.3 | 7.0 | 0.3 | 4.8 | −25.1 | 13.8 | |
| ***Average*** | ***2.3±0.2*** | ***6.8±2.0*** | ***1.0±0.9*** | ***6.5±3.1*** | ***−24.7±1.3*** | ***14.8±3.0*** | |
| PE12 | 4.0 | 6.4 | 0.2 | 3.0 | −22.7 | 13.9 | 6 |
| PE11 | 2.2 | 6.7 | 1.6 | 5.1 | −23.4 | 13.4 | |
| PE1 | 4.4 | 6.0 | 1.9 | 10.1 | −24.1 | 17.5 | |
| PE13 | 3.2 | 4.0 | 0.0 | 1.5 | −24.5 | 16.3 | |
| ***Average*** | ***3.5±1.0*** | ***5.8±1.2*** | ***0.9±1.0*** | ***4.9±3.8*** | ***−23.7±0.8*** | ***15.3±2.0*** | |
| PE15 | 10.5 | 5.7 | 3.1 | 13.4 | −25.4 | 14.6 | 5 |
| PE14 | 3.8 | 5.6 | 7.6 | 16.7 | −22.7 | 11.4 | |
| PE9 | 2.1 | 7.1 | 6.1 | 17.1 | −23.6 | 13.0 | |
| PE10 | 5.0 | 7.7 | 3.9 | 15.6 | −22.8 | 11.4 | |
| PE8 | 2.8 | 7.3 | 10.8 | 18.2 | −24.1 | 12.7 | |
| PE2 | 6.9 | 8.1 | 7.6 | 16.1 | −23.7 | 11.7 | |
| PE3 | 5.0 | 7.7 | 19.5 | 24.2 | −23.1 | 11.5 | |
| ***Average*** | ***5.2±2.8*** | ***7.0±1.0*** | ***8.4±5.5*** | ***17.3±3.4*** | ***−23.6±0.9*** | ***12.3±1.2*** | |
| PE7 | 4.8 | 6.5 | 13.5 | 20.9 | −23.5 | 17.7 | 4 |
| PE6 | 5.8 | 7.7 | 17.8 | 22.8 | −23.5 | 14.6 | |
| PE39 | 4.0 | 2.6 | 21.7 | 28.0 | −23.8 | 9.3 | |
| PE4 | 4.8 | 4.6 | 25.1 | 29.9 | −23.9 | 11.1 | |
| PE5 | 4.0 | 8.6 | 23.2 | 26.9 | −23.3 | 12.3 | |
| PE40 | 3.0 | 2.7 | 15.8 | 24.9 | −23.9 | 9.0 | |
| ***Average*** | ***4.4±1.0*** | ***5.5±2.5*** | ***19.5±4.5*** | ***25.6±3.4*** | ***−23.6±0.2*** | ***12.3±3.3*** | |
| PE33 | 20.0 | 1.2 | 31.0 | 32.1 | −24.1 | 10.3 | 3 |
| PE35 | 14.0 | 1.9 | 29.8 | 31.2 | −22.2 | 19.6 | |
| PE34 | 11.0 | 2.3 | 29.3 | 31.3 | −24.1 | 10.1 | |
| PE37 | 20.0 | 1.9 | 28.6 | 30.9 | −23.2 | 10.4 | |
| PE36 | 5.0 | 1.3 | 29.2 | 31.1 | −22.8 | 9.0 | |
| PE38 | 8.0 | 1.9 | 28.6 | 30.9 | −22.8 | 12.3 | |
| ***Average*** | ***13.0±6.2*** | ***1.8±0.4*** | ***29.4±0.9*** | ***31.3±0.4*** | ***−23.2±0.8*** | ***12.0±3.9*** | |
| PE27 | 14.0 | 2.7 | 32.8 | 32.1 | −21.8 | 7.7 | 2 |
| PE26 | 14.0 | 2.1 | 32.8 | 32.1 | −21.0 | 7.1 | |
| PE30 | 35.0 | 2.4 | 32.4 | 31.8 | −23.2 | 9.0 | |
| PE31 | 8.0 | 2.8 | 29.1 | 31.7 | −21.8 | 7.8 | |
| PE29 | 8.0 | 2.6 | 30.9 | 31.8 | −22.3 | 8.8 | |
| PE28 | 14.0 | 2.0 | 33.0 | 32.2 | −22.5 | 10.0 | |
| PE32 | 6.0 | 1.9 | 30.7 | 32.0 | −21.9 | 8.0 | |
| ***Average*** | ***14.1±9.8*** | ***2.4±0.4*** | ***31.7±1.5*** | ***32.0±0.2*** | ***−22.1±0.7*** | ***8.3±1.0*** | |
| PE21 | 24.0 | 2.0 | 33.7 | 32.8 | −21.0 | 6.8 | 1 |
| PE24 | 31.0 | 2.6 | 33.7 | 33.2 | −21.1 | 7.1 | |
| PE22 | 25.0 | 2.0 | 33.8 | 33.1 | −20.8 | 6.8 | |
| PE25 | 21.0 | 1.6 | 33.7 | 33.2 | −21.5 | 8.0 | |
| PE23 | 28.0 | 2.3 | 33.8 | 33.2 | −21.2 | 6.5 | |
| ***Average*** | ***25.8±3.8*** | ***2.1±0.4*** | ***33.7±0.1*** | ***33.1±0.2*** | ***−21.1±0.3*** | ***7.0±0.6*** | |

**Table 2** AMS radiocarbon dates from benthic foraminifera

| Lab code | Depth (cm) | Sample no. | $^{13}C/^{12}C$ (‰) | Radiocarbon age (yr BP) | Calibrated age 2 sigma (yr BP) |
|---|---|---|---|---|---|
| Beta-193746 | 200–205 | HKV37200 | −2.5 | 3470±40 | 3440–3260 |
| Beta-193747 | 290–295 | HKV37290 | −1.5 | 4330±40 | 4540–4370 |
| Beta-193748 | 700–705 | HKV37700 | −2.9 | 7020±40 | 7570–7430 |
| Beta-193749 | 970–975 | HKV37970 | −1.7 | 7970±40 | 8500–8350 |

particle size distribution for the core was also analysed at the same sampling interval using a laser granulometer. The chronology of the core is based on four AMS radiocarbon dates of benthic foraminifera measured by Beta Analytic Inc. (Table 2). The dates were calibrated to calendar years using the program CALIB 4.3 and the data base MARINE98 (Stuiver *et al.*, 1998).

Diatom samples were prepared using standard methods (Palmer and Abbott, 1986), and diatoms were counted under a light microscope with 1000× magnification and minimum 300 valves per sample counted. The counts were displayed using the TILIA package (Grimm, 1993) and expressed as percentage of total diatom valves (%TDV). Diatom species were classified into salinity groups including polyhalobous (fully marine), mesohalobous (brackish water), oligohalobous halophile (salt-tolerant freshwater), oligohalobous indifferent (freshwater) and halophilous (salt-intolerant freshwater), according to Denys (1991–92) and Round *et al.* (1990). CONISS was applied to group diatom counts, using the stratigraphically unconstrained method for the present-day surface samples and the stratigraphically constrained method for the core samples.

For bulk organic carbon isotopes, total organic carbon and nitrogen measurements all samples were treated with 5% HCl to remove carbonates, washed and dried before homogenization in an agate pestle and mortar. Percentage carbon and nitrogen were measured using a Carlo Erba elemental analyser, calibrated through an internal standard. Replicate analyses of samples gave a precision of $< \pm 0.1\%$ at one standard deviation. Because the errors are so small, error bars are not shown in the diagrams. The $^{13}C/^{12}C$ analyses were performed by combustion using a Carlo Erba 1500 online to a VG Triple Trap and Optima dual-inlet mass spectrometer. The $\delta^{13}C$ values were calculated to the VPDB scale using a within-run laboratory standard calibrated against NBS-19 and NBS-22. Replicate analyses of samples gave precision of $\pm 0.1$‰.

## Results: the modern environment

According to the diatom results, the 40 surface sediment samples can be divided into seven groups (Figure 4) with group 1 being most distal from the freshwater source and

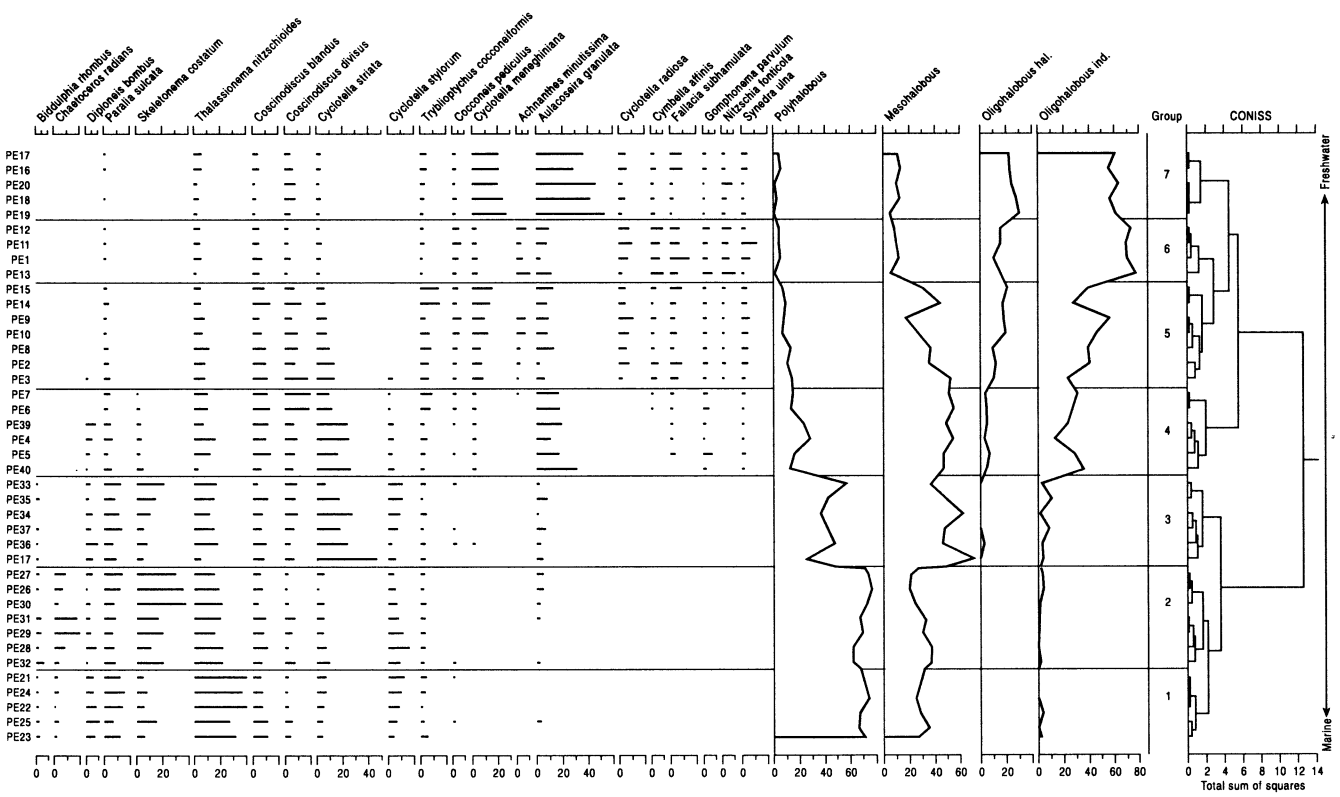


**Figure 4** Diatom flora for the 40 present-day surface sediment samples, only taxa with over 5% of total diatom count shown. The samples are ordered based on the result of the cluster analysis using CONISS of the diatom data. Locations of samples and distribution of groups are shown in Figure 2

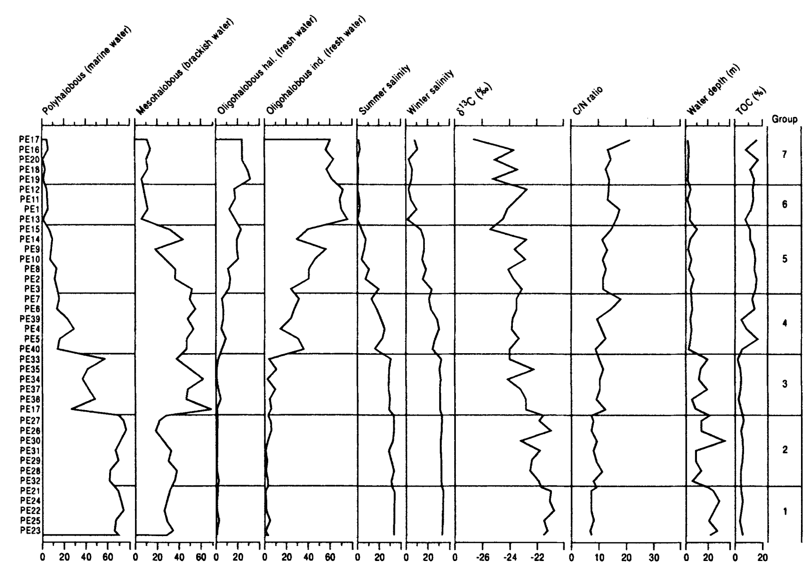


**Figure 5** Environmental variables (water salinity, water depth, TOC, C/N ratios and $\delta^{13}C$ values) and summary diatom data from the modern sediment samples collected from the Pearl River Estuary

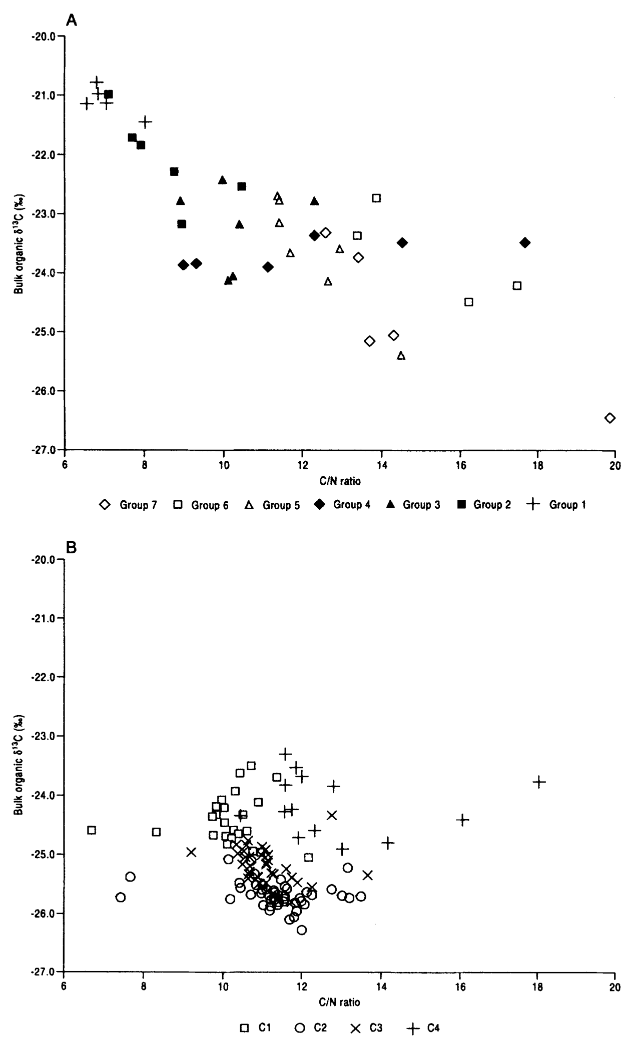


**Figure 6** Bi-plots of $\delta^{13}C$ values and C/N ratios. (A) Shows the bi-plot from present-day surface samples. The different groups identified in Figure 4 are represented by different symbols. (B) Shows the bi-plot of data from the sediment core. The four zones identified in the core, C1, C2, C3 and C4 (from 990–830 cm, 830–410 cm, 410–150 cm and 150–0 cm, respectively) are represented by different symbols. The standard deviation for each data point is smaller than $\pm 0.1$ for both $\delta^{13}C$ values and C/N ratios

group 7 being most proximal to freshwater source (Figure 2). Environmental variables of water depth and water salinity, TOC, C/N ratios and $\delta^{13}C$ values for these samples are listed in Table 1 and plotted in Figure 5, while their locations are shown in Figure 2. A plot of $\delta^{13}C$ versus C/N for individual data points is shown in Figure 6A, with group average values presented in Figure 7. Generally speaking, water depths of groups 1 to 3 are deeper, (5 to 35 m), whilst for groups 4 to 7 depths range between 2 m and 7 m. Water salinity is highest in group 1 and lowest in group 7. Diatom assemblages are closely related to the trend of water salinity. TOC values are below 3% in groups 1 to 3, and mostly over 5% in groups 4–7. The C/N ratios increase from group 1 to group 7. There is also a clear trend in the $\delta^{13}C$ values – higher in group 1 and lower in group 7. A close relationship between the diatom data, C/N ratios, organic $\delta^{13}C$ values and the environmental variables of salinity, water depth and TOC content can be seen in Figure 5. The following sections will present in more detail the relationship between diatom flora, C/N ratios and the range of $\delta^{13}C$ values.

Group 1 includes sites furthest from the Pearl River, southeast of Hong Kong (Figure 2), where water salinity is slightly higher in summer (33.7‰) than in winter (33.1‰) because of evaporation. These sites are typical of marine environments with limited freshwater influence. This group has the highest average salinity of all seven groups, and also the deepest average water depth of 25.8 m. The diatom assemblages are dominated by marine species, especially *Thalassionema nitzschioides* along with *Paralia sulcata* and *Diploneis bombus* (Figure 4). This group of sediment samples has the lowest C/N average ratios of $7.0 \pm 0.6$ and the highest mean $\delta^{13}C$ value at $-21.1 \pm 0.3$‰ (Figure 7). This is consistent with the main source of organic carbon being from marine algae.

Group 2 is also distal from the Pearl River (Figure 2). The environment is close to fully marine water conditions but there is some influence from monsoon freshwater flux in summer, with water salinity being slightly lower in summer (31.7‰) than in winter (32.0‰). The limited freshwater influence is likely to come from the Pearl River Estuary and small streams of Hong Kong Island and Lantau Island, which will reduce summer surface water salinity. The diatom assemblages are dominated by marine planktonic taxa, including *Chaetoceros radians, Skeletonema*

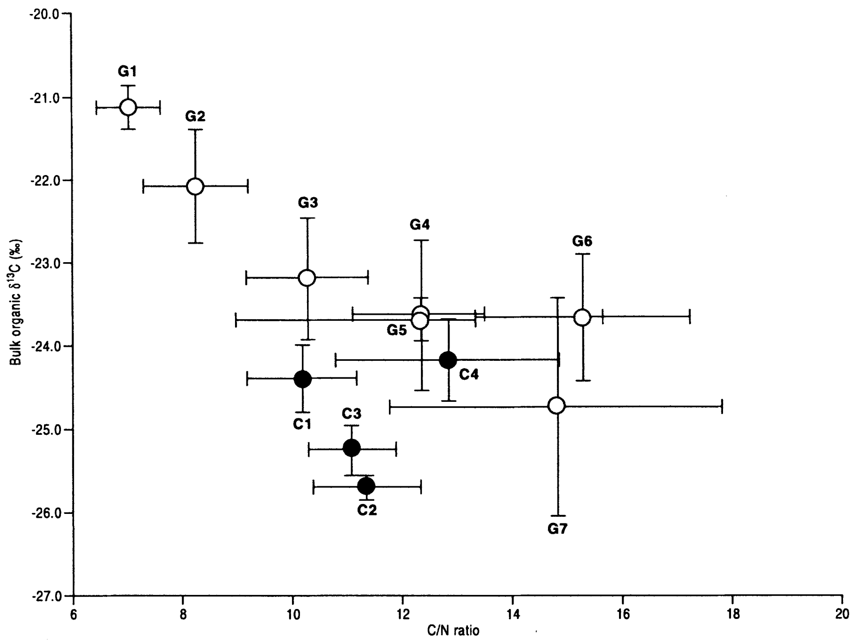


**Figure 7** Summary bi-plot of $\delta^{13}C$ values and C/N ratios for the surface sample groups (G1 to G7) and for the sediment core zones (C1 to C4). The values plotted are group/zone means with 1 standard deviation error bars

*costatum* and *Thalassionema nitzschioides*. The average C/N ratio is $8.3 \pm 1.0$ and average $\delta^{13}C$ value for this group is $-22.1 \pm 0.7‰$ (Figure 7), suggesting that the source of organic carbon for this group is mainly marine aquatic plants such as algae.

Group 3 is composed of samples collected from the northwest of Hong Kong, closer to the Pearl River than groups 1 and 2. This area records an average salinity of 31.2‰, but with a weak influence from the monsoon flux of freshwater from the Pearl River in summer, when water salinity drops to 29.4‰ on average. The diatom assemblages are dominated by brackish water taxa with a high proportion of marine taxa. The most common diatom species in this group is *Cyclotella striata*, which can tolerate a wide range of salinity. The average C/N ratio is $12.0 \pm 3.9$ and the mean $\delta^{13}C$ value is $-23.2 \pm 0.8‰$, suggesting that the source of organic carbon is mainly from marine aquatic plants, but may involve some freshwater aquatic plants and even some terrestrial plants.

Group 4 comprises samples from the eastern section of the estuary. This area is influenced by stronger flood tides but weaker ebb tides. Water salinity here ranges from 19.5‰ in summer to 25.6‰ in winter, which is typical of a brackish water environment. The significantly lowered summer water salinity reflects a strong monsoon flux of freshwater. The diatom assemblages are characterized by the presence of diatoms from all salinity groups. They are dominated by brackish water taxa (*Coscinodiscus blandus, Cos. dividus* and *Cyclotella striata*), but also freshwater diatoms, such as *Aulacoseira granulata*, as well as marine diatoms, *Thalassionema nitzschioides* are present. The C/N ratios ($12.3 \pm 3.3$) are higher than groups 1 to 3. The average $\delta^{13}C$ value is $-23.6 \pm 0.2‰$, significantly lower than values for groups 1 and 2, but with some overlap with values of group 3 (Table 1). The evidence suggests a mixture of sources of organic carbon for this group, as expected in mid-estuary.

Group 5, from sites within the central and inner part of the estuary, is strongly influenced by both flood and ebb tides as well as variations of freshwater flux. Water salinity here is much lower than groups 1 to 4, ranging from 8.4‰ in summer to 17.3‰ in winter. This represents a brackish environment strongly affected by seasonal changes in freshwater flux. The diatom results show mixed assemblages, although freshwater taxa are more abundant. The average C/N ratio is $12.3 \pm 1.2$ and the mean $\delta^{13}C$ value is $-23.6 \pm 0.9‰$, showing a significant overlap with group 4 and partial overlap with groups 3 and 6 (Figure 7), all from the inner part of the estuary, suggesting a mixture of carbon sources.

Group 6 is composed of samples from a tributary with one sample just beyond the mouth. These sites are dominated by freshwater conditions during the majority of the year with a minor influence of tidal water during winter. Accordingly, water salinity in summer is as low as 0.9‰ and in winter reaches only 4.9‰. The diatom assemblages are dominated by freshwater taxa, many of them benthic types. The average C/N ratio for this group is $15.3 \pm 2.0$, with a mean $\delta^{13}C$ value of $-23.7 \pm 0.8‰$. Despite the overlapping $\delta^{13}C$ values, the C/N ratios are significantly higher than those of group 5. The high C/N ratios and $\delta^{13}C$ values suggest the main source of organic carbon is from freshwater aquatic plants with some input from terrestrial plants (which have high C/N ratios).

Group 7 is composed of sites within the main tidal channel of the estuary, which is occupied by freshwater for most of the year. Water salinity varies between 1.0‰ in summer and 6.5‰ in winter. The diatom assemblages are characterized by two dominant species, *Cyclotella meneghiniana* and *Aulacoseira granulata*, both are freshwater planktonic diatoms. The average C/N ratio is $14.8 \pm 3.0$ and the mean $\delta^{13}C$ value is $-24.7 \pm 1.3‰$. The significantly higher $\delta^{13}C$ values and C/N ratios reflect the dominantly freshwater environment.

In summary, modern samples from the Pearl River estuary show a strong relationship between diatom flora, C/N ratios, organic carbon isotopic values and water salinity. The zonation based on the diatom data identifies seven groups

**Table 3** Lithology of core V37 (seabed altitude: 1.5 m below mean sea level)

| Depth (cm) | Sediment descriptions |
|---|---|
| 0–15 | Sediment lost during retrieval |
| 15–200 | Very soft to soft, dark greenish grey, slightly sandy clayey silt with occasional shell fragments (marine deposits) |
| 200–600 | Soft, dark greenish grey, clayey silt with occasional shell fragments (marine deposits) |
| 600–1010 | Soft to firm, dark greenish grey, clayey silt with occasional shell fragments (marine deposits) |
| 1010–1060 | Firm, dark grey, clayey silt with subrounded fine gravels and light brown clay pockets (transitional layer) |
| 1060–1340 | Soft to firm, light yellowish brown and spotted light red silt and clay (alluvial deposits) |

covering the transition from fully marine conditions (group 1) in the southeastern distal margins to the study area, through brackish water conditions in the outer section of the estuary (groups 2, 3 and 4), to near fully freshwater conditions in the inner section of the estuary (groups 5, 6 and 7). The higher organic content (TOC values) in groups 4, 5, 6 and 7 coincides with their shallower water and closeness to the freshwater source. Despite some overlapping in $\delta^{13}C$ values and C/N ratios, the seven groups correspond well with their dominant sources of organic carbon, which are related to the varying influence of monsoonal freshwater flux.

These results suggest that a combination of diatom, C/N and organic carbon isotope techniques can be used to aid reconstruction of the history of freshwater flux, which can be related to change in monsoon climate. Diatoms are sensitive to water salinity, which varies according to freshwater influence. Variations in $\delta^{13}C$ values and C/N ratios can be used to infer variations in the strength of monsoonal freshwater flux.

## Results: the sediment core

The upper 10 m section of the sediment core (V37) was analysed for particle size, diatom, C/N and organic carbon isotopes. Below 1060 cm (Table 3) is a section of desiccated sediments of pre-Holocene age (Yim *et al.*, 1990; Yim and Tovey, 1995). Above the transitional layer between 1060 cm and 1010 cm is a marine unit containing dark greenish grey clayey silt commonly referred to as unit M1 in the Quaternary marine and terrestrial sequences (Yim and Li, 2000) and Hang Hau Formation (Fyfe *et al.*, 1999). The calibrated age–depth model based on the four AMS radiocarbon dates (Table 1) suggests steady sedimentation at a rate of 1.47 mm/yr.

The analysis of particle size distribution (Figure 8) shows the sediments are mainly fine grained in the lower part of the core below 300 cm, suggesting a hydrodynamically quiet environment. Between 300 cm and 200 cm, there are several thin layers of coarser sediment. In the top 200 cm, the sediments become slightly sandier. The increase of coarser sediments in the upper part of the core may be a result of the site becoming shallower, as a result of sediment infill, and influenced by stronger hydrodynamic conditions.

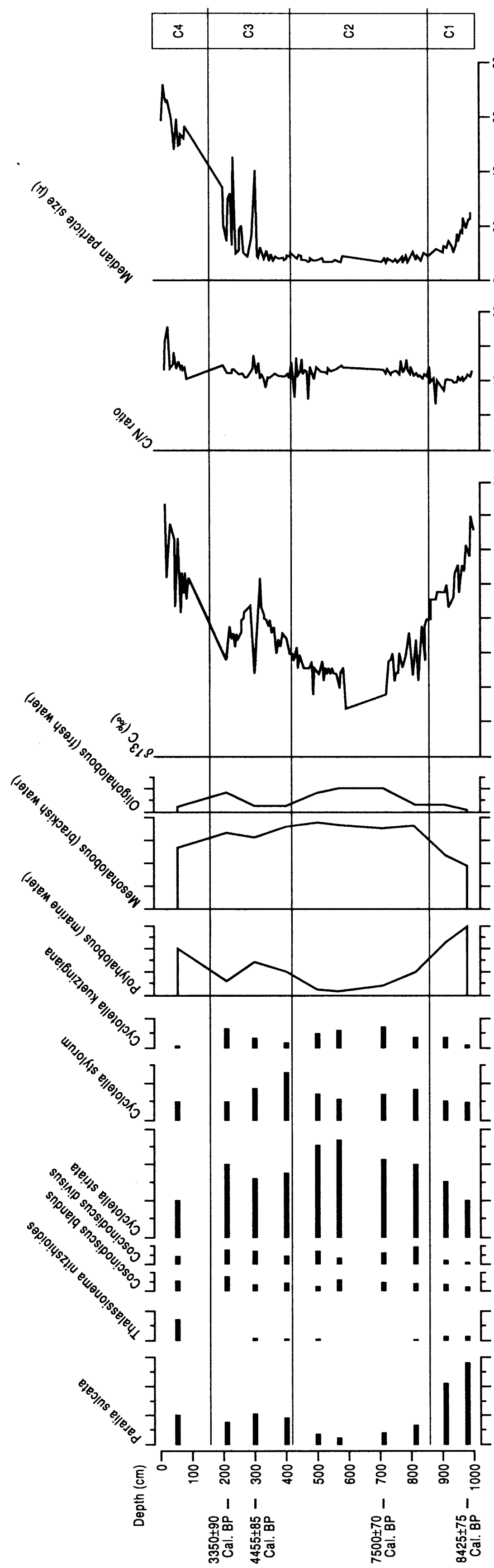


**Figure 8** Results of analysis from sediment core, diatom flora, $\delta^{13}C$ values, C/N ratio and median particle size. Diatoms shown are taxa over 5% of total diatom count. The errors for both $\delta^{13}C$ and C/N measurement are too small (lower than $\pm 0.1\%$) to be plotted on the curves. The ages are calibrated radiocarbon dates (see Table 3)

## Diatoms

Based on the diatom data from core V37, four zones (Figure 8) can be identified from the stratigraphically constrained cluster analysis. Zone 1 from the base of the core to 830 cm shows a decrease in *Paralia sulcata*, a marine planktonic species and an increase in brackish water taxa, particularly *Cyclotella striata*, indicating an increase in freshwater influence. Zone 2 is dominanted by brackish water taxa but with freshwater taxa becoming more common. In terms of salinity preferences, the change in diatom flora from zone 1 to zone 2 in the core is similar to the change from group 2 to group 4 seen in the modern samples. Zone 3 sees a significant increase in marine diatoms. Zone 4 is characterized by a continued increase in marine diatoms. Based on the published diatom salinity tolerances and the modern data from the Pearl River Estuary, trends in salinity variation can be reconstructed over the past 8500 years. Therefore, diatom data from the core suggest a change in water salinity from near fully marine conditions at base of the core (8425 $\pm$ 75 cal. yr BP) to brackish water conditions at 700 cm (7500 $\pm$ 70 cal. yr BP). Brackish-freshwater conditions were sustained at the core site from 700 to 500 cm (*c.* 7000–6000 cal. yr BP). The top 400 cm of the core, since *c.* 5200 cal. yr BP, is characterized by fluctuating and generally increased water salinity.

The diatom data from the base of the core indicate near fully marine conditions. This is supported by evidence of a postglacial marine transgression through palaeo-valleys into the deltaic basin well before 9500 cal. yr BP (Owen *et al.*, 1998). By the time the core site was inundated around 8500 cal. yr BP, the core site was already distal to the source of freshwater. By 7500 cal. yr BP, relative sea level reached $-5$ m and continued to rise at a reduced rate thereafter (Zong, 2004). As a typical postglacial deltaic response, rising sea level would normally result in a shoreline retreat, putting the core site in a more distal position. If the volume of freshwater flux remains constant, an increase in water salinity would be expected. However, the diatom flora from the core shows a reduction in water salinity. A possible explanation for the decrease in water salinity during a period of sea-level rise is that freshwater flux, possibly with sediment supply, increased significantly and diluted the influence of sea-level rise on water salinity. This is supported by Li *et al.* (1991), who show that diatom records from sediment cores from the inner sector of the Pearl River estuary record a phase of strong freshwater flux dated to 8500–6500 cal. yr BP, with the flux being much stronger than at the present day.

The diatom flora suggest an increase in marine influence from approximately 500 cm (*c.* 6000 cal. yr BP) produced either by a decline in freshwater flux or by a rise in sea level, or a combination of both (Figure 8). This period of increased marine influence and reduced freshwater flux persisted until 300 cm (4455 $\pm$ 85 cal. yr BP). Zong (2004) has shown that relative sea level continued to rise from 7000 to 3000 cal. yr BP but at a reduced rate. Therefore, the increase in marine influence recorded in core V37 is likely a result of the combined effects of a reduction in freshwater flux and the continued rise in sea level.

The diatom flora from the upper section of the core suggest a further increase in marine influence after a brief interval of increased freshwater flux at 200 cm (3350 $\pm$ 90 cal. yr BP). This corresponds to a period of relative sea-level fall identified by Zong (2004) from 0.8 m above present. Therefore, the increase in marine influence is most likely due to a reduction in freshwater flux. Furthermore, during the last 1000 years human activity within the Pearl River basin has intensified, leading to an increase in sedimentation and seaward migration of the shoreline (eg, Li *et al.*, 1991). This shoreline migration acts to increase the proximity of the core site to the source of freshwater, which should lead to a decrease in salinity. However, water salinity in the mouth of the estuary has not reduced, implying a weakening of the freshwater flux.

## C/N and $\delta^{13}C$ results

The organic carbon $\delta^{13}C$ values and C/N ratios for the core are plotted together in Figure 6B, summarized in Figure 7 and plotted against depth in Figure 8. The majority of the core samples have C/N ratios between 10 and 12 (Figure 6B), suggesting that the majority of organic carbon in the sediment is from aquatic plants (eg, Meyers, 1994). The $\delta^{13}C$ values from the core concentrate between $-24.0‰$ and $-26.0‰$. These values tend to be lighter (or lower) than the values from modern samples (Figure 7). The C/N ratios are generally stable throughout the core, despite a few data points that deviate from the mean (Figure 8). There is a weak trend towards the top of the core where C/N ratios reach over 18. However, there is a significant range of $\delta^{13}C$ values through the core. The $\delta^{13}C$ values at the base of the core between 990 cm and 970 cm are around $-24.0‰$, indicative of a brackish water environment. The $\delta^{13}C$ values become significantly lower from 970 cm to 700 cm, suggesting an increase in freshwater-sourced organic carbon input. Between the same depths, the C/N ratios rise slightly from 10 to 11.5, implying an increase in vascular detritus. From 700 cm to 500 cm, the $\delta^{13}C$ values remain stable at around $-25.5$ to $-26.0‰$, with an average C/N ratio of 11.7, pointing to a freshwater carbon source. From 500 cm, the $\delta^{13}C$ values become progressively higher, implying an increase in marine-sourced organic carbon input, albeit with a degree of variability. The top of the core, zone 4, has $\delta^{13}C$ values suggesting a mix of marine and freshwater organic carbon sources. The increasing C/N ratios at the top of the core suggest an increase in the supply of vascular organic matter. The trends seen in the $\delta^{13}C$ and C/N ratio results from the core match very well with the trends identified from the diatom results, showing (1) an increase in freshwater flux from 8425 $\pm$ 75 cal. yr BP to 7500 $\pm$ 70 cal. yr BP, (2) a period of strong freshwater flux in the middle Holocene and (3) a weakening freshwater flux from the middle to late Holocene.

Despite showing similar trends there are minor differences between the diatom and organic carbon records. The diatom results suggest changes from marine-brackish water conditions in the early and late Holocene and brackish-freshwater conditions in middle Holocene. The $\delta^{13}C$ results suggest a change between a mixed organic carbon source indicative of brackish water conditions in the early and late Holocene and a predominantly freshwater source in the middle Holocene (suggesting reduced marine influence compared with the diatom flora). As Figure 7 shows, there appears to be an offset between the $\delta^{13}C$ values from the core and the modern samples. This offset is highlighted by the diatom data (as outlined above). For example, the sediment sample from 980 cm yields a $\delta^{13}C$ value of $-23.6‰$ and a diatom assemblage equivalent to group 2 of the modern sample set (Figure 5). Yet, the modern samples of group 2 have an average $\delta^{13}C$ value of $-22.1 \pm 0.7‰$ (Table 1), 1.5‰ higher than the fossil sample. Similarly, the sediment sample from 502 cm has a $\delta^{13}C$ value of $-25.8‰$ and a diatom assemblage equivalent to group 4 of the modern sample set. Samples from group 4 have an average

$\delta^{13}C$ value of $-23.6 \pm 0.2‰$, a difference of 2.2‰ from the fossil data.

As summarized in Figure 7, there is a general offset in $\delta^{13}C$ values between the modern samples and the core samples, despite overlapping C/N ratios. It is possible that the $\delta^{13}C$ values of bulk organic carbon from the core may have been lowered by approximately 2.0‰ because of diagenetic processes. Several studies have reported lower $\delta^{13}C$ values (between 2.0‰ and 4.0‰) in Holocene coastal sediments compared with modern-equivalent sediments (DeLaune, 1986; Fogel *et al.*, 1989; Wilson *et al.*, 2005). The C/N ratios from the core are mostly between 10 and 14 (Figure 6B), suggesting that there is a certain amount of vascular detritus in the sediment samples. Thus, the selective preservation of cellulose and lignin of vascular plant detritus in these samples may be responsible for the slightly lower $\delta^{13}C$ values (eg, Deines, 1980; Benner *et al.*, 1987; Chmura and Aharon, 1995).

## The Holocene monsoon history

The diatom, C/N and organic carbon isotope data from the core reveal a certain degree of variability in freshwater flux during the past 8500 years. We interpret this variability as reflecting changes in monsoonal strength. The reconstructed monsoon history presented here mirrors other records from the Pearl River basin as well as other parts of China. Our data show an increase in freshwater flux from 8500 cal. yr BP, culminating in a period of strong monsoonal freshwater flux between 7500 and 6000 cal. yr BP (Figure 8). This is supported by pollen records from the Pearl River basin indicating a period of warm and wet climate during this period (Huang *et al.*, 1982; Li *et al.*, 1991). Elsewhere, lake records from western Tibet (Gasse *et al.*, 1991) and Yunnan, southwest China (Hodell *et al.*, 1999) suggest the summer monsoon regime was greatly intensified from the beginning of the Holocene. This period was also characterized by significant increase in temperature in eastern China (Feng *et al.*, 1993). The western Loess Plateau was relatively wet between 8300 and 7400 cal. yrs BP and distinctly humid and warm between 7400 and 6700 cal. yr BP (An *et al.*, 2004), implying a climate with strong summer monsoon, during which the desert–loess transitional zone moved northward by three degrees of latitude (Zhou *et al.*, 2002).

The gradual decline in freshwater flux from 6000 cal. yr BP revealed by diatom and $\delta^{13}C$ data from the core (Figure 8) is also supported by pollen records from the Pearl River basin. The changes coincide with the Neoglacial climate cooling and a period of cool and dry climate dominating southern China (Huang *et al.*, 1982), and a period of reduced precipitation in the Pearl River drainage basin (Li *et al.*, 1991). Zhang *et al.* (2004) have reconstructed a climatic record from a stalagmite in a cave within the Pearl River basin covering the last 6000 years. Their evidence suggests that the strong East Asian summer monsoon gradually weakened from 6000 cal. yr BP associated with a decrease in precipitation. Initially this weakening coincided with a climate in southern China that was still warm and relatively humid during the interval from 6000 to 3800 cal. yr BP. The period from 3800 to 373 cal. yr BP, however, was characterized by a cool climate as the East Asian summer monsoon continued to weaken (Zhang *et al.*, 2004). In northern China, a widespread weakening in the strength of the summer monsoon is evident for a short period from 5000 to 4500 cal. yr BP (Morrill *et al.*, 2003). This is the period when marine influence in the Pearl River Estuary was greatly increased, indicated by both diatom and organic carbon isotope data (around 300 cm, Figure 8). Also from northern and eastern China, stable isotope records (eg, Hou *et al.*, 2003) indicate a progressively dryer climate for the last 1000 years. This supports the interpretation of an increase in marine influence in the top section of our core (Figure 8) relating to a decline in freshwater flux associated with a weakening of monsoon precipitation.

## Conclusions

In this paper we have analysed the distribution of diatom assemblages, C/N ratios and values of organic carbon isotopes in the modern environment of the Pearl River Estuary. The results show a strong relationship between water salinity, diatom assemblages, C/N ratios and $\delta^{13}C$ values in the modern environment. There is a significant relationship between organic carbon isotope values and water salinity, which implies that organic carbon sources (freshwater or marine) may be established by examining C/N ratios and $\delta^{13}C$ values from estuarine sediments. Water salinity and the sources of organic carbon in an estuarine environment can be linked to freshwater flux and/or marine influence, therefore both the diatom and organic carbon isotopic techniques can be used to reconstruct changes in freshwater flux associated with palaeo-monsoonal changes. The two techniques applied to a sediment core obtained from the mouth of the Pearl River Estuary are in reasonable agreement. Both reveal an increase in freshwater flux from *c.* 8500 to *c.* 6000 cal. yr BP, followed by a general decrease in freshwater flux during the last 6000 years.

Diatom assemblages are closely related to water salinity, yet $\delta^{13}C$ values are dependent on the combined sources of organic carbon and are independent of water salinity. Therefore, the organic carbon isotope technique is a useful environmental proxy, independent of other proxies such as diatoms. Both techniques provide an indirect measure of freshwater flux, however, the diatom technique tends to be labour-intensive and time-consuming, while the organic carbon isotope technique is much faster and thus allows high-resolution sampling. In addition some brackish water diatom taxa have wide salinity tolerances and, as a result, the reconstruction may lose precision. Therefore, the combination of the two techniques may be the best way to achieve high-resolution and accurate reconstructions of palaeo-monsoonal history.

## Acknowledgements

This research was supported by the University of Durham through a special research grant awarded to Y. Zong, and by the Research Grants Council of the Hong Kong Special Administrative Region, China, through research grants HKU7024/03P and HKU7051/04P awarded to W.W.-S. Yim. The authors thank the director of the Environmental Protection Department, HK SAR Government for the collection of surface sediment samples and water salinity, the director of the Civil Engineering Department, HK SAR Government for the collection of the sediment core. Jo Green and Carol Arrowsmith are thanked for help with the isotope data, and the Imaging and Design Unit, Department of Geography, University of Durham for the production of the diagrams. This manuscript was also improved by the constructive comments of Dr Andrew Plater, Professor Michael Bird and an anonymous reviewer.

# Appendix 1

The ecological characteristics of major diatom species (over 5% TDV) identified from surface sediment samples obtained from the Pearl River Estuary and the waters around Hong Kong

| Species | Authority | Salinity class | Life form |
|---|---|---|---|
| *Achnanthes minutissima* | (Kütz.) Cleve | Oligohalobous (ind.) | Benthic |
| *Aulacoseira granulata* | (Ehr.) Simonson | Oligohalobous (ind.) | Planktonic |
| *Biddulphia rhombus* | (Ehre.) W. Smith | Polyhalobous | Planktonic |
| *Chaetoceros radians* | Schütt | Polyhalobous | Planktonic |
| *Cocconeis pediculus* | Ehrenberg | Oligohalobous (hal.) | Benthic |
| *Coscinodiscus blandus* | A. Schmidt | Mesohalobous | Planktonic |
| *Coscinodiscus divisus* | Grunow | Mesohalobous | Planktonic |
| *Cyclotella Kuetzingiana* | Thwaites | Oligohalobous (ind.) | Planktonic |
| *Cyclotella meneghiniana* | Kützing | Oligohalobous (hal.) | Planktonic |
| *Cyclotella radiosa* | (Grun.) Lemmerman | Oligohalobous (ind.) | Planktonic |
| *Cyclotella striata* | (Kütz.) Grunow | Mesohalobous | Planktonic |
| *Cyclotella stylorum* | Brightwell | Mesohalobous | Planktonic |
| *Cymbella affinis* | Kützing | Oligohalobous (ind.) | Benthic |
| *Diploneis bombus* | (Ehre.) Ehrenberg | Polyhalobous | Benthic |
| *Fallacia subhamulata* | D.G. Mann | Oligohalobous (ind.) | Benthic |
| *Gomphonema parvulum* | (Kütz.) Kützing | Oligohalobous (ind.) | Benthic |
| *Nitzschia fonticola* | Grunow | Oligohalobous (ind.) | Benthic |
| *Nitszchia sigma* | (Kütz.) A. Smith | Mesohalobous | Benthic |
| *Paralia sulcata* | (Ehre.) Cleve | Polyhalobous | Planktonic |
| *Skeletonema costatum* | (Greville) Cleve | Polyhalobous | Planktonic |
| *Synedra ulna* | (Nitz.) Ehrenberg | Oligohalobous (ind.) | Benthic |
| *Thalassionema nitschioides* | (Grun.) Grunow | Polyhalobous | Planktonic |
| *Tryblioptychus cocconeiformis* | (Cleve) Hendey | Mesohalobous | Planktonic |

# References


**An, C., Feng, Z.** and **Tang, L.** 2004: Environmental change and cultural response between 8000 and 4000 cal. yr BP in the western Loess Plateau, northwest China. *Journal of Quaternary Science* 19, 529–35.

**An, Z., Porter, S.C., Zhou, W., Lu, Y., Donahue, D.J., Head, M.J., Wu, X., Ren, J.** and **Zheng, H.** 1993: Episode of strengthened summer monsoon climate of Younger Dryas age on the loess plateau of Central China. *Quaternary Research* 39, 45–54.

**Benner, R., Fogel, M.L., Sprague, K.E.** and **Hodson, R.E.** 1987: Depletion of $^{13}$C in lignin and its implications for stable carbon isotope studies. *Nature* 329, 708–10.

**Boutton, T.W.** 1991: Stable carbon isotope ratios of natural materials: II. Atmospheric, terrestrial, marine and freshwater environments. In Coleman, D.C. and Fry, B., editors, *Carbon isotope techniques.* Academic Press, 173–85.

**Bryne, R., Ingram, L.B., Starratt, S., Malamus-Roam, F., Collins, J.** and **Conrad, M.** 2001: Carbon-isotope, diatom and pollen evidence for Late Holocene salinity change in a brackish marsh in the San Francisco Estuary. *Quaternary Research* 55, 66–76.

**Burns, S.J., Matter, A., Frank, N.** and **Mangini, A.** 1998: Speleothem based paleoclimate record from northern Oman. *Geology* 26, 499–502.

**Chen, F.-H., Shi, Q.** and **Wang, J-M.** 1999: Environmental changes documented by sedimentation of Lake Yiema in arid China since the late glaciation. *Journal of Paleolimnology* 22, 159–69.

**Chmura, G.L.** and **Aharon, P.** 1995: Stable carbon isotope signatures of sedimentary carbon in coastal wetlands as indicators of salinity regime. *Journal of Coastal Research* 11, 124–35.

**Chu, G., Liu, J., Sun, Q., Lu, H., Gu, Z., Wang, W.** and **Liu, T.** 2002: The 'Mediaeval Warm Period' drought recorded in Lake Huguangyan, tropical south China. *The Holocene* 12, 511–16.

**Deines, P.** 1980: The isotopic composition of reduced organic carbon. In Fritz, P., and Fontes, J.C., editors, *Handbook of environmental isotope geochemistry.* Gisewir, 329–406.

**DeLaune, R.D.** 1986: The use of $\delta^{13}$C signature of $C_3$ and $C_4$ plants in determining past depositional environments in rapidly accreting marshes of the Mississippi River deltaic plain, Louisiana, U.S.A. *Chemical Geology* 59, 315–20.

**Denniston, R.F., Gonzalez, L.A., Asmeron, Y., Sharma, R.H.** and **Reagan, M.K.** 2000: Speleothem evidence of changes in Indian summer monsoon precipitation over the last ~2300 years. *Quaternary Research* 53, 196–202.

**Denys, L.** 1991/92: *A check-list of the diatoms in the Holocene deposits of the western Belgian coastal plain with a survey of their apparent ecological requirements.* Professional Paper 1991–2 No. 246, De Lescluzestraat, 68, B-2600 Berchem, Belgium.

**Feng, X., Cui. H., Tang, K.** and **Conkey, L.E.** 1999: Tree-ring δD as an indicator of Asian Monsoon intensity. *Quaternary Research* 51, 262–66.

**Feng, Z., Thompson, L.G., Mosley-Thompson, E.** and **Yao, T.** 1993: Temporal and spatial variations of climate in China during the last 10,000 years. *The Holocene* 3, 174–80.

**Fogel, M.L., Sprague, K.E., Gize, A.P.** and **Frey, R.W.** 1989: Diagenesis of organic matter in Geogeia salt marshes. *Estuarine, Coastal and Shelf Science* 28, 211–30.

**Fontugne, M.R.** and **Jouanneau, J.M.** 1987: Modulation of the particulate organic carbon flux to the ocean by a macrotidal estuary – evidence from measurements of carbon isotopes in organic matter from the Gironde Estuary. *Estuarine Coastal and Shelf Science* 24, 377–87.

**Fyfe, J.A., Selby, I.C., Plater, A.J.** and **Wright, M.R.** 1999: Erosion and sedimentation associated with the last sea-level rise offshore Hong Kong, South China Sea. *Quaternary International* 55, 93–100.

**Gasse, F., Arnold, M., Fontes, J.C., Fort, M., Gilbert, E., Huc, A., Li, B., Li, Y., Liu, Q., Melieres, F., Van Campo, E., Wang, F.** and

**Zhang, Q.** 1991: A 13,000-year climate record from western Tibet. *Nature* 353, 742–45.

**Grimm, E.C.** 1993: *TILIA: a pollen program for analysis and display.* Illinois State Museum.

**Hodell, D.A., Brenner, M., Kanfoush, S.L., Curtis, J.H., Stoner, J.S., Song, X., Wu, Y.** and **Whitmore, T.J.** 1999: Paleoclimate of southwestern China for the past 50,000 yr inferred from lake sediment records. *Quaternary Research* 52, 369–80.

**Hou, J., Tan, M., Cheng, H.** and **Liu, T.** 2003: Stable isotope records of plant cover change and monsoon variation in the past 2200 years: evidence from laminated stalagmites in Beijing, China. *Boreas* 32, 304–13.

**Huang, C.-Y., Liew, P.-M., Zhao, M., Cheng, T-C., Kuo, C-M., Chen, M-T., Wang, C-H.** and **Zheng, L-F.** 1997: Deep sea and lake records of the southeast Asian paleomonsoons for the last 25 thousand years. *Earth and Planetary Science Letters* 146, 59–72.

**Huang, Z., Li, P., Zhang, Z., Li, K.** and **Qiao, P.** 1982. *Zhujiang Delta* (in Chinese). General Scientific Press.

**Lamb, A.L., Leng, M.J., Umer, M.** and **Lamb, H.F.** 2004: Holocene climate and vegetation change in the Main Ethiopian Rift Valley, inferred from the composition (C/N and $\delta^{13}C$) of lacustrine organic matter. *Quaternary Science Reviews* 23, 881–91.

**Leng, M.J.** and **Marshall, J.D.** 2004: Palaeoclimate interpretation of stable isotope data from lake sediment archives. *Quaternary Science Reviews* 23, 811–31.

**Li, P., Qiao, P., Zheng, H., Fang, G.** and **Huang, G.** 1991: *The environmental evolution of the Pearl River Delta in the last 10,000 years.* China Ocean Press (in Chinese).

**Lister, G.S., Kelts, K., Chen, K., Yu, J.** and **Niessen, F.** 1991: Lake Qinghai, China: closed-basin lake levels and oxygen isotope record for ostracoda since the latest Pleistocene. *Palaeogeography, Palaeoclimatology, Palaeoecology* 84, 141–62.

**Lou, J.-Y.** and **Chen, C-T.A.** 1997: Paleoclimatology and paleoenvironmental records since 4000 BP in sediments of alpine lakes in Taiwan. *Science in China* 40, 424–31.

**Mackie, E.A.V., Leng, M.J., Lloyd, J.M.** and **Arrowsmith, C.** 2005: Bulk organic $\delta^{13}C$ and C/N ratios as palaeosalinity indicators within a Scottish isolation basin. *Journal of Quaternary Science* 20, 303–12.

**Meyers, P.A.** 1994: Preservation of elemental and isotopic source identification of sedimentary organic matter. *Chemical Geology* 114, 289–302.

**Meyers, P.A.** and **Ishiwatari, R.** 1993: Organic matter accumulation records in lake sediment. In Lerman, A., Imboden, D. and Gat, J., editors, *Physics and chemistry of lakes.* Springer, 279–328.

**Meyers, P.A.** and **Teranes, J.L.** 2001: Sediment organic matter. In Last, W.M. and Smol, J.P., editors, *Tracking environmental change using lake sediments volume 2. Physical and chemical techniques.* Kluwer Press, 239–69.

**Middelburg, J.J.** and **Nieuwenhuize, J.** 1998: Carbon and nitrogen stable isotopes in suspended matter and sediments from the Schelde Estuary. *Marine Chemistry* 60, 217–25.

**Morrill, C., Overpeck, J.T.** and **Cole, J.E.** 2003: A synthesis of abrupt changes in the Asian summer monsoon since the last deglaciation. *The Holocene* 13, 465–76.

**Müller, A.** 2001: Late- and postglacial sea-level change and paleoenvironments in the Oder Estuary, southern Baltic Sea. *Quaternary Research* 55, 86–96.

**Müller, A.** and **Mathesius, U.** 1999: The palaeoenvironments of coastal lagoons in the southern Baltic Sea I: the application of sedimentary $C_{org}/N$ ratios as source indicators of organic matter. *Palaeogeography, Palaeoclimatology, Palaeoecology* 145, 1–16.

**Müller, A.** and **Voss, M.** 1999: The palaeoenvironments of coastal lagoons in the southern Baltic Sea, II: $\delta^{13}C$ and $\delta^{15}N$ ratios of organic matter – sources and sediments. *Palaeogeography, Palaeoclimatology, Palaeoecology* 145, 17–32.

**Overpeck, J., Anderson, D., Trumbore, S.** and **Prell, W.** 1996: The southwest Indian monsoon over the past 18,000 years. *Climate Dynamics* 12, 213–25.

**Owen, R.B.** 2005: Modern fine-grained sedimentation – spatial variability and environmental controls on an inner pericontinental shelf, Hong Kong. *Marine Geology* 214, 1–26.

**Owen, R.B., Neller, R.J., Shaw, R.** and **Cheung, P.C.T.** 1998: Late Quaternary environmental changes in Hong Kong. *Palaeogeography, Palaeoclimatology, Palaeoecology* 138, 151–73.

**Palmer, A.J.M.** and **Abbott, W.H.** 1986: Diatoms as indicators of sea-level change. In van de Plassche, O., editor, *Sea-level research: a manual for the collection and evaluation of data.* Geo Books, 457–87.

**Round, F.E., Crawford, R.M.** and **Mann, D.G.** 1990: *The diatoms: biology and morphology of the genera.* Cambridge University Press.

**Sarkar, A., Ramesh, R., Somayajulu, B.L.K., Agnihotri, R., Jull, A.J.T.** and **Burr, G.S.** 2000: High resolution Holocene monsoon record from the eastern Arabian Sea. *Earth and Planetary Science Letters* 177, 209–18.

**Shukla, J.** and **Paolina, D.A.** 1983: The Southern Oscillation and longrange forcasting of the summer monsoon rainfall over India. *Monthly Weather Review* 111, 1830–37.

**Sirocko, F., Garbe-Shonberg, M., McIntyre, A.** and **Molfino, B.** 1996: Teleconnections between the subtropical monsoons and high-latitude climates during the last deglaciations. *Science* 272, 526–29.

**Smith, B.N.** and **Epstein, S.** 1971: Two categories of $^{13}C/^{12}C$ ratios for higher plants. *Plant Physiology* 47, 380–84.

**Stuiver, M., Reimer, P.J., Bard, E., Beck, J.W., Burr, G.S., Hughen, K.A., Kromer, B., McCormac, G., van der Plicht, J.** and **Spurk, M.** 1998: INTCAL98 radiocarbon calibration, 24,000–0 cal BP. *Radiocarbon* 40, 1041–83.

**Thompson, L.G., Mosley-Thompson, E., Davis, M.E., Bolzan, J.F., Dai, J., Yao, T., Gundestrup, N., Wu, X., Klein, L.** and **Xie, Z.** 1989: Holocene–Late Pleistocene climatic ice core records from Qinghai–Tibetan Plateau. *Science* 246, 474–77.

**Thompson, L.G., Yao, T., Mosley-Thompson, E., Davis, M.E., Henderson, K.A.** and **Lin, P.N.** 2000: A high-resolution millennial record of South Asian monsoon from Himalayan ice cores. *Science* 289, 1916–19.

**Thornton, S.F.** and **McManus, J.** 1994: Application of organic carbon and nitrogen stable isotope and C/N ratios as source indicators of organic matter provenance in estuarine systems: evidence from the Tay estuary, Scotland. *Estuarine, Coastal and Shelf Science* 38, 219–33.

**Wang, L., Sarnthein, M., Erlenkeuser, H., Grootes, P.M., Grimalt, J.O., Pelejero, C.** and **Linck, G.** 1999a: Holocene variations in Asian monsoon moisture: a bidecadal sediment record from the South China Sea. *Geophysical Research Letters* 26, 2889–92.

**Wang, L., Sarnthein, M., Grootes, P.M.** and **Erlenkeuser, H.** 1999b: Millennial occurrence of century scale abrupt events of East Asian monsoon: a possible heat conveyor for the global deglaciation. *Paleoceanography* 14, 725–31.

**Westman, P.** and **Hedenström, A.** 2002: Environmental changes during isolation processes fomr the Litorina Sea as reflected by diatoms and geochemical parameters – a case study. *The Holocene* 12, 531–40.

**Wilson, G.P., Lamb, A.L., Leng, M.J., Gonzalez, S.** and **Huddart, D.** 2005: $\delta^{13}C$ and C/N as potential coastal palaeoenvironmental indicators in Mersey Estuary, U.K. *Quaternary Science Reviews* 24, 2015–29.

**Yamamuro, M.** 2000: Chemical tracers of sediment organic matter origins in two coastal lagoons. *Journal of Marine Systems* 26, 127–34.

**Yang, S.** 1996: ENSO-snow-monsoon associations and seasonal-interannual predictions. *International Journal of Climatology* 14, 739–50.

**Yim, W.W.-S.** and **Li, J.** 2000: Diatom preservation in an inner continental shelf borehole from the South China Sea. *Journal of Asian Earth Sciences* 18, 471–88.

**Yim, W.W.-S.** and **Tovey, N.K.** 1995: Desiccation of inner continental shelf sediments during Quaternary low sea-level stands. *Geoscientist* 5/4, 34–35.

**Yim, W.W.-S., Ivanovich, M.** and **Yu, K.F.** 1990: Young age bias of radiocarbon dates in pre-Holocene marine deposits of Hong Kong and implications for Pleistocene stratigraphy. *Geo-Marine Letters* 10, 165–72.

**Zhang, M., Yuan, D., Lin, Y., Qin, J., Bin, L., Cheng, H.** and **Edwards, R.L.** 2004: A 6000-year high-resolution climatic record

froma stalagmite in Xiangshui Cave, Guilin, China. *The Holocene* 14, 697–702.
**Zhou, W., Dodson, J., Head, M.J., Li B., Hou, Y.J., Lu, X., Donahue, D.J.** and **Jull, Aw.J.T.** 2002: Environmental variability within the Chinese desert–loess transitional zone over the last 20,000 years. *The Holocene* 12, 107–12.
**Zong, Y.** 1992: Postglacial stratigraphy and sea-level changes in the Han River delta, China. *Journal of Coastal Research* 8, 1–28.
—— 2004: Mid-Holocene sea-level highstand along southeast coast of China. *Quaternary International* 177, 55–67.